

See discussions, stats, and author profiles for this publication at: <https://www.researchgate.net/publication/353248006>

# Anthropogenic and climatic driven peatland degradation during the past 150 years in Greater Khingan Mountains, NE China

Article in *Land Degradation and Development* · July 2021

DOI: 10.1002/ldr.4036

CITATIONS

0

READS

66

7 authors, including:



**Dongxue Han**

Chinese Academy of Sciences

19 PUBLICATIONS 99 CITATIONS

[SEE PROFILE](#)



**Chuanyu Gao**

Chinese Academy of Sciences

50 PUBLICATIONS 465 CITATIONS

[SEE PROFILE](#)



**Hanxiang Liu**

Chinese Academy of Sciences

16 PUBLICATIONS 86 CITATIONS

[SEE PROFILE](#)



**Li Yunhui**

Chinese Academy of Sciences

10 PUBLICATIONS 49 CITATIONS

[SEE PROFILE](#)

Some of the authors of this publication are also working on these related projects:



Landscape evolution of watershed wetlands during the last century [View project](#)





A study on the resilience of the typical lakeside wetland ecosystem under climate change based on records of plant macrofossils and carbon accumulation in the southeastern Tibetan Plateau over the last millennium [View project](#)

## RESEARCH ARTICLE

WILEY

# Anthropogenic and climatic-driven peatland degradation during the past 150 years in the Greater Khingan Mountains, NE China

Dongxue Han<sup>1</sup> | Chuanyu Gao<sup>1</sup>  | Hanxiang Liu<sup>2</sup> | Yunhui Li<sup>1</sup> | Jinxin Cong<sup>1</sup> | Xiaofei Yu<sup>1,3</sup> | Guoping Wang<sup>1</sup> 

<sup>1</sup>Key Laboratory of Wetland Ecology and Environment, Northeast Institute of Geography and Agroecology, Chinese Academy of Sciences, Changchun, PR China

<sup>2</sup>Key Laboratory of Alpine Ecology, Institute of Tibetan Plateau Research, Chinese Academy of Sciences, Beijing, PR China

<sup>3</sup>School of Environment, Northeast Normal University, Changchun, PR China

## Correspondence

Guoping Wang, Key Laboratory of Wetland Ecology and Environment, Northeast Institute of Geography and Agroecology, Chinese Academy of Sciences, Changchun 130102, PR China.

Email: wangguoping@neigae.ac.cn

## Funding information

China Postdoctoral Science Foundation, Grant/Award Number: 2020M681059; Department of Science and Technology of Jilin Province, Grant/Award Number: 20190101011JH; Fundamental Research Funds for the Central Universities, Grant/Award Number: 2412019BJ003; Ministry of Science and Technology of the People's Republic of China, Grant/Award Number: 2016YFA0602301; National Natural Science Foundation of China: 41911530188; Youth Innovation Promotion Association of the Chinese Academy of Sciences, Grant/Award Number: 2020235

## Abstract

Relationships between modern pollen, climate, and human activities are important for improving the explanation of fossil records. To better understand anthropogenic and climatic impact on peatland vegetation and environment, we assessed the impact of the human influence index (HII) on modern pollen assemblages from 61 surface soil samples (different land-use types) in the Greater Khingan Mountains by using detrended correspondence analysis and redundancy analysis. Based on the palynological analysis, <sup>210</sup>Pb age-depth model, and weighted averaging partial least squares, we reconstructed HII values of Tuqiang peatland in the Greater Khingan Mountains during the last 150 years. The reconstructed HII values demonstrated that the intensity of human activities increased gradually before 1900 AD, when the population of Heilongjiang Province was less and its native inhabitants continued to hunt and gather. During the period of 1900–1950 AD, human influence intensity increased sharply and reached peak values. Wars and placer gold mining caused large numbers of people immigrated north to Heilongjiang Province, rapid population growth strengthened the human impact intensity. In addition, invaders exploited the forest resources without limit. Widescale deforestation and land reclamation destroyed vegetation landscape and reduced forest coverage seriously, which led to soil erosion and land degradation. With the foundation of new China (1949 AD), the implementation of forest protection policies clearly reduced the human disturbance intensity. However, due to the needs of economic development, human influence intensity increased again after 2000 AD.

## KEYWORDS

Human Influence Index, land use, peatland degradation, pollen, quantitative reconstruction

## 1 | INTRODUCTION

With the rapid population expansion, human activities are pervasive in most ecosystems around the world, which have led to unprecedented destruction to natural vegetation and have become a major driving force of terrestrial ecosystem change

since the industrial revolution era (Cheng et al., 2018; X. Q. Li, et al., 2009; M. Y. Li et al., 2015; Shu et al., 2010). The 'Anthropocene' is considered to be a new human-dominated geological epoch (although not yet fully formally established) owing to the intensified human influence on Earth ecosystems (Crutzen, 2002; Crutzen & Stoermer, 2000).

Human activities and climate change are two crucial drivers that varied terrestrial ecosystem (J. Y. Li et al., 2013; Mackenzie et al., 2018; H. Zhang et al., 2015), but the interaction (or relative contribution) of the two factors is debated (H. Y. Liu et al., 2006; H. Zhang et al., 2015). Modern climate data have been recorded by instrumental observations during the recent decades. To quantify the intensity of human disturbance, a global modern Human Influence Index (HII) dataset is developed; the spatial resolution of this dataset is 1 km<sup>2</sup> (Sanderson et al., 2002). The dataset is created by integrating several indices, which could reflect human influence intensity, including human population density, infrastructure (land use/cover, nighttime lights, and build-up areas), and accessibility (such as roads, railroads, coastlines, and navigable rivers). In palaeoecological researches, this HII dataset makes it possible to quantitatively reconstruct the intensity of human influence (J. Y. Li et al., 2014; M. Y. Li et al., 2015). Research on past human–nature interaction has significant implications not only for exploring the long-term human civilization but also for further assess to the current environment dynamics in the case of longer-term human disturbance (Shu et al., 2010).

During the last century, the annual mean temperature of surface air has risen by 1.3°C in the Amur River basin (Novorotskii, 2007). The Greater Khingan Mountains, are located in the northern high-latitude region, are highly sensitive to climate change and currently experience an amplified warming than other regions in the world (Melles et al., 2019; H. Zhang et al., 2018; C. Zhao et al., 2015). Also, the Greater Khingan Mountains have a high proportion of forests and peatlands cover (Gao et al., 2018). While human activities have led to degradation and disappearance of extensive peatlands, which have seriously affected the balance of ecosystem. At the beginning of 1900 AD, people from other regions (e.g., Southern China) began to immigrate to or invade (such as Japan and Russia) Northeast China, the forest resources were exploited without limit in the Greater Khingan Mountains (G. Z. Liu, 2001). After 1950 AD, the Government of China paid more attention to forest resources protection and began to control the intensity of exploitation (G. Z. Liu, 2001). Enhanced human influence had led to a rapid reduction of forests and peatlands area, which damaged ecosystem function seriously. Thus, an understanding of historical vegetation change and human disturbance in the Greater Khingan Mountains is necessary.

The Greater Khingan Mountains are one of the crucial peatland distribution regions in China; the area of peatlands is nearly 42,450 km<sup>2</sup> (Gao et al., 2018; Xing et al., 2015). Peatlands have continuous deposition inputs and slow decomposition rates under anaerobic environment (Gao et al., 2018). Peats are regarded as one of the faithful geological archives of past climate change and human activities, which deposit in situ, have a high resolution, and record continuously. They reliably register environmental variation and peatland development process, as well as climate and human activities history, and have a great potential for reconstruction of palaeovegetation, palaeoenvironment, and palaeoclimate. Pollen in peat sediments can provide direct information on vegetation composition. Palynological analysis has been commonly applied worldwide to quantitatively reconstruct historical variability of vegetation and climate (J. Y. Li

et al., 2017; Stebich et al., 2015; Xu et al., 2010; Y. Zhao et al., 2010; C. Zhao et al., 2015). Comparatively few palaeoenvironmental records are available on the relationships between historical vegetation and human, especially in Northeast China (J. Y. Li et al., 2013; Mackenzie et al., 2018).

In the present study, we use the modern HII and WorldClim datasets, combined with the pollen assemblages of 61 surface soil samples from different land-use types (including 42 wetlands, 10 forests, 7 grasslands, and 2 residences) in the Greater Khingan Mountains, in order to discuss the relationships between modern pollen assemblages, human activities, and climate, and further to understand the impacts of historical human activities and climate change on peatland vegetation variation. Our specific aims were: (1) to assess the effect of HII on the abundance of pollen taxa from modern surface soil samples by using detrended correspondence analysis (DCA) and redundancy analysis (RDA); (2) to establish and evaluate the transfer function of modern pollen-HII by employing WA-PLS; (3) based on <sup>210</sup>Pb age-depth model, to reconstruct the historical HII values quantitatively in Tuqiang peatland; and (4) to discuss the impact of human activities and climate on historical variation of vegetation compared with other proxies in the Greater Khingan Mountains during the last 150 years.

## 2 | MATERIALS AND METHODS

### 2.1 | Study area and sampling

The study area is situated in the Greater Khingan Mountains (48.79–53.50° N, 121.51°–128.47° E). The area belongs to a cold temperate continental monsoon climate. The mean annual temperature (Tann) here is –4°C, the average temperature in January is about –29°C, and winter is long, dry, and cold from November to April. The average temperature in July is about 18°C, summer is short, wet, and hot between June and August. The mean annual precipitation (Pann) amounts to 452 mm; more than 80% of the rainfall occurs between May and September (Fick & Hijmans, 2017; Han et al., 2019).

A total of 61 surface soil samples were collected from different land-use types (including 42 wetlands, 10 forests, 7 grasslands, and 2 residences) in the Greater Khingan Mountains in July 2017 (Figure 1a) (Han et al., 2020). Samples were collected from 0–1 cm deep surface soil, to reduce sampling error, 5 points within a 3 m × 3 m sampling plot were mixed together. Longitude, latitude, and altitude were recorded by GPS at each sampling site. Detailed site information was shown in Table S1.

Tuqiang profile (TQ1, 52.94°N, 122.85°E, altitude 474 m above sea level) in the Greater Khingan Mountains was collected in November 2016 (Figure 1b,c). Dominant species in Tuqiang peatland are consisted of shrubs (*Betula fruticosa*, *Ledum palustre*, *Vaccinium uliginosum*, *Chamaedaphne calyculata*, *Salix myrtilloide*), sedges (*Eriophorum vaginatum*), and moss (*Sphagnum magellanicum*, *Sphagnum capillifolium*), surrounded by *Larix gmelinii*, *Betula platyphylla* forests on all sides, and a few trees of the same species grow in the site (Han

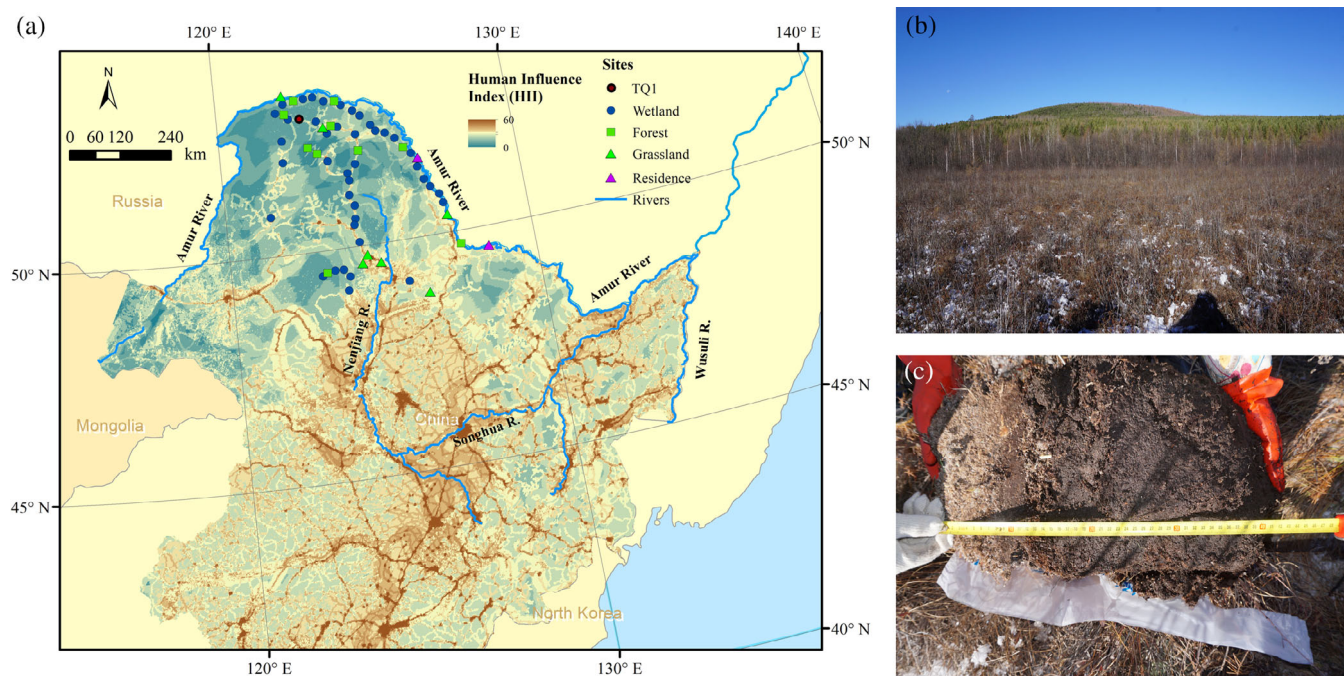


**FIGURE 1** (a) Location of sampling sites from different land-use types in the Greater Khingan Mountains; (b) the picture of Tuqiang peatland; and (c) a picture of TQ1 profile [Colour figure can be viewed at [wileyonlinelibrary.com](http://wileyonlinelibrary.com)]

et al., 2019). The total length of TQ1 profile was 40 cm, and the profile can be subdivided into three sections: peat with roots (0–10 cm), light brown peat (11–25 cm), and dark brown peat (26–40 cm). Samples were sliced continuously at 1-cm interval in the field, packed, taken back to laboratory, and stored at 4°C prior to analysis.

## 2.2 | Modern HII and climate data

To quantify the intensity of human disturbance, a global modern dataset of HII is developed with a spatial resolution of 1 km<sup>2</sup> (Sanderson et al., 2002; WCS/CIESIN, 2005). HII values range from 0 to 64, have been obtained by integrating several indices which reflect human influence intensity, for instance, human population density, infrastructure (land use/cover, nighttime lights, and build-up areas), and accessibility (coastlines, roads, railroads, and navigable rivers). HII values of each sampling site were derived from the modern HII dataset. Modern site-specific climate data was extracted from the WorldClim dataset with a spatial resolution of 1-km (Fick & Hijmans, 2017). Two key climate parameters (Tann and Pann) were used in this study.

## 2.3 | <sup>210</sup>Pb dating

Subsamples (1-cm interval) were dried at 105°C in an oven for 12 hr, ground into powder with a mortar and filled the plastic quasi-cylindrical bottle (7 ml) up (H. X. Liu et al., 2019). After 3 weeks storage in sealed containers to allow radioactive equilibrium, total <sup>210</sup>Pb,

<sup>214</sup>Pb, and <sup>214</sup>Bi radioactivities were measured using a low background gamma spectroscopy with a high pure Ge semiconductor (ORTEC Instruments Ltd., USA). The radioactivity of <sup>226</sup>Ra, which represents the supported <sup>210</sup>Pb, was calculated using the mean value of <sup>214</sup>Pb and <sup>214</sup>Bi (Van Cleef, 1994). A 40,000 s counting time was set to ensure the measurement precision at the 95% level of confidence. The standard radioactive sources with known reference dates and activities used to calibrate detectors absolute efficiencies were supplied by National Institute of Metrology, China (<sup>210</sup>Pb: 1.39e + 02 Bq, 2016-06-08; <sup>226</sup>Ra: 3.83E + 01 Bq, 2016-06-05). The age-depth framework was established through the constant rate of supply model (Appleby & Oldfield, 1978). The detailed <sup>210</sup>Pb dating results of TQ1 profile were shown in published article (Cong et al., 2019).

## 2.4 | Pollen analysis

Pollen pretreatment followed the conventional HCl-NaOH-HF methods (Fægri & Iversen, 1989). At the beginning of chemical processing, a tablet of *Lycopodium* spore (27,560 grains spores) was added in each sample for calculating absolute pollen concentrations (grains/g). Pollen was identified and counted using a light microscope (Olympus BX-53) at 400 times magnification, with the aid of pollen atlases published by Wang et al. (1995) and Tang et al. (2016). We identified and counted more than 400 terrestrial pollen grains (from a minimum of three to four slides) for each sample. The total sum of terrestrial pollen species was used for pollen percentages calculations, while the percentages of ferns spores were calculated based on the sum of terrestrial pollen plus ferns spores (Y. Zhao et al., 2010). We

draw pollen assemblages diagram using Tilia software (version 1.7.16) and divided the pollen assemblage zones employing constrained cluster analysis (CONISS).

## 2.5 | Numerical analyses

Multivariate ordinations were applied to investigate the relationships between pollen assemblages and environmental variables using CANOCO 4.5 software (Ter Braak & Smilauer, 2003). To reduce the bias owing to the presence of rare pollen taxa, we selected 16 pollen taxa (percentage > 5%, occurred in at least three samples) for numerical analyses. Pollen percentages data of each sample were transformed into square root. The gradient length of the first axis in DCA was 1.653, which was less than 3, suggesting the use of linear-based RDA (Ter Braak & Prentice, 1988). The statistical significance of each variable (HII, Tann, and Pann) was evaluated by Monte Carlo permutation tests (999 random permutations).

The weighted averaging partial least squares (WA-PLS) (Ter Braak & Juggins, 1993) were selected to establish transfer function between modern pollen composition and environmental variable using C2 software (version 1.7.7). The pollen abundances were standardized and transformed into their square roots (27 pollen taxa were selected, minimum percentage > 1%, occurrences > 3 times). The statistical

testing was performed using leave-one-out cross-validation (Dixit et al., 1993; Ma et al., 2018). The evaluation of transfer function was based on root-mean-square error of prediction (RMSEP), coefficient of determination ( $r^2$ ) between observed and predicted values, and maximum bias (max. bias) in residuals. The appropriate WA-PLS component was selected using random  $t$ -test (van der Voet, 1994). The model with low RMSEP, high  $r^2$ , low maximum bias, and the smallest number of 'useful' component is the ideal candidate.

## 3 | RESULTS

### 3.1 | Modern pollen assemblages and HII values

In total, 40 pollen taxa including 10 trees, 3 shrubs, and 27 herbs were identified in 61 surface soil samples from different land-use types (Figure 2). Trees are mainly consisted of *Betula*, *Pinus*, *Larix*, and *Alnus*; shrubs are mainly from Ericaceae and Rosaceae; herbs are dominated by Cyperaceae, *Artemisia*, Chenopodiaceae, and Poaceae.

In wetlands, Cyperaceae (average 17.4%) is the dominant pollen type, but the content of *Artemisia* (average 7.8%), Poaceae (average 3.3%), Chenopodiaceae (average 2.3%), and *Sanguisorba* (average 1.1%) are also relatively higher. Trees pollen types are mainly *Betula* (average 38.9%), *Pinus* (average 11.7%), *Alnus* (average 5.5%), *Larix*

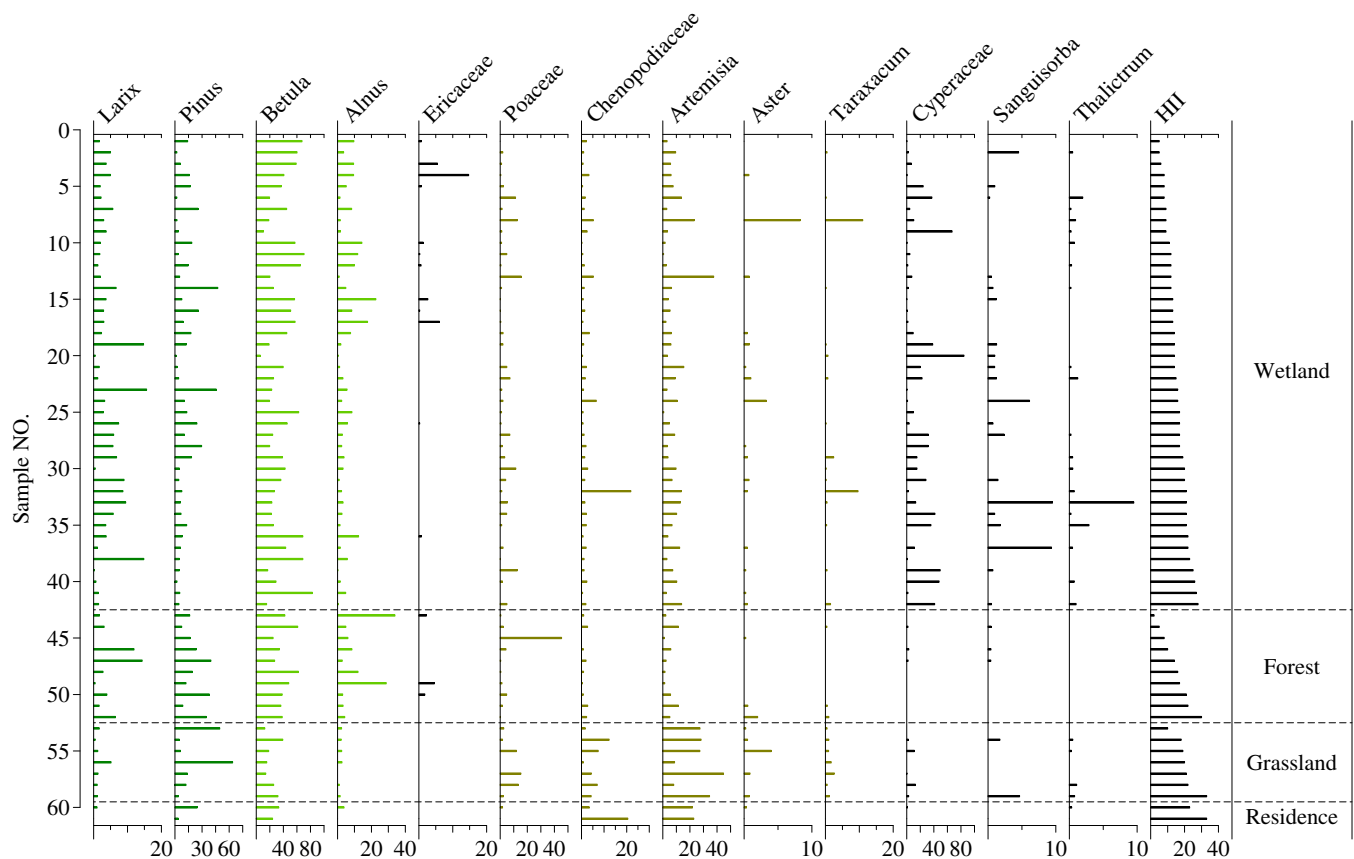


**FIGURE 2** Pollen percentage diagrams of 61 surface soil samples (42 wetlands, 10 forests, 7 grasslands, and 2 residences). Only the main taxa were shown [Colour figure can be viewed at [wileyonlinelibrary.com](http://wileyonlinelibrary.com)]



(average 4.4%), and *Quercus* (average 1.5%). The shrubs are consisted of Rosaceae (average 1.0%) and Ericaceae (average 0.8%). The percentages of arboreal and herbaceous pollen taxa are 63.3% and 34.8%, respectively.

In forests, the content of trees is 83.1%, which is dominated by *Betula* (average 41.3%), *Pinus* (average 21.7%), *Alnus* (average 10.8%), *Larix* (average 4.6%), *Quercus* (average 2.5%), *Salix* (average 1.3%), and so on. Shrubs pollen is about 2.0%, mainly Rosaceae (average 1.0%) and Ericaceae (average 0.9%). Herbs are dominated by Poaceae (average 6.1%), *Artemisia* (average 4.9%), and Chenopodiaceae (average 1.4%).

In grasslands, herbs percentage is 47.6%, mainly composed of *Artemisia* (average 25.6%), Poaceae (average 6.8%), Chenopodiaceae (average 5.4%), and Cyperaceae (average 4.2%). Trees pollen percentage is 51.9%, mainly *Betula* (average 22.6%), *Pinus* (average 22.0%), *Alnus* (average 1.8%), *Larix* (average 1.7%), and *Quercus* (average 1.7%).

In residences, the percentage of trees is 49.2%; trees pollen is predominated by *Betula* (average 28.7%), *Pinus* (average 14.1%), *Quercus* (average 3.5%), *Alnus* (average 1.9%), and *Salix* (average 0.5%). Herbs percentage is 49.4%, mainly composed of *Artemisia* (average 22.3%), Chenopodiaceae (average 12.0%), and Poaceae (average 0.9%).

The average HII values are 15, 14, and 20 in wetlands, forests, and grasslands, respectively, which indicate low human influence intensity in the natural vegetation types. While the human impact intensity is higher in the human-induced vegetation types, the average HII value is 28 in residences.

### 3.2 | Ordination analyses and calibration model

The DCA results based on 16 selected main pollen taxa (minimum percentage > 5%, occurrences >3-times) and the total number of surface soil samples showed that the first axis and the second axis explained 16% and 7%, respectively, altogether accounted for 23% of the total variance in pollen assemblages. To better estimate the relationship between modern pollen assemblages and environmental variables of different land-use types in the Greater Khingan Mountains, the linear RDA model was selected based on the gradient length of first axis in DCA (the gradient length of first axis was 1.653, less than 3). We selected 16 main pollen taxa (the same as in DCA) and 3 environmental variables (HII, Tann, and Pann) in RDA analysis.

RDA results (Figure 3) indicated that HII, Tann, and Pann were all significantly related to the sample scores in axis 1 and axis 2 (eigenvalues were 0.203 and 0.014, respectively). The Monte Carlo permutation tests (999 unrestricted permutations) showed HII, Tann, and Pann were all statistically significant at the 95% level ( $p < 0.05$ ). The inflation factor of each variable was lower than 2 indicating that the degree of collinearity among HII, Tann, and Pann was low. HII, Tann, and Pann were all positively correlated with axis 1, with coefficients 0.28, 0.76, and 0.40, respectively. Tann and Pann were positively correlated with axis 2 ( $r = 0.02$  and  $0.25$ , respectively), whereas HII was negatively correlated with axis 2 ( $r = -0.20$ ). In addition, the results

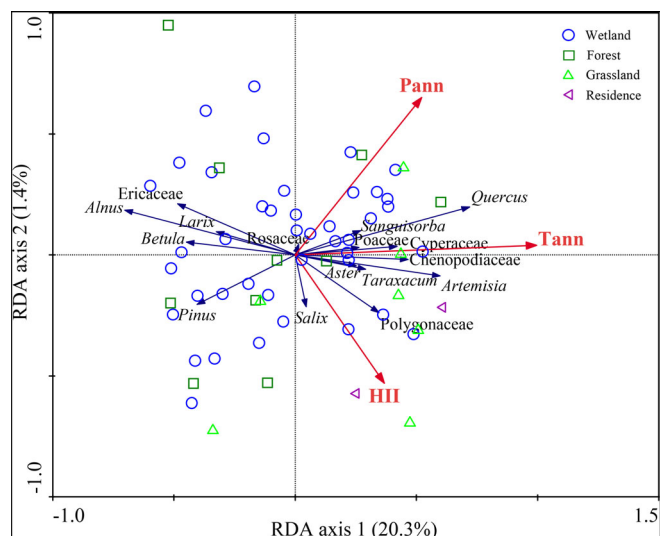


**FIGURE 3** Biplots of redundancy analysis (RDA) results based on 16 main pollen taxa and 61 surface soil samples [Colour figure can be viewed at [wileyonlinelibrary.com](http://wileyonlinelibrary.com)]

of the forward selection procedure suggested that all HII, Tann, and Pann were statistically significant in relation to the variance of modern pollen data ( $\lambda = 0.0125, 0.2014, \text{ and } 0.0124$ , respectively), indicating that modern HII-pollen dataset exhibited in our study was useful for quantitatively reconstructing HII values.

Based on DCA and RDA analyses, the WA-PLS calibration model was applied to establish quantitative relationship between surface pollen samples and modern HII values. A total of 27 pollen taxa were selected (minimum percentage > 1%, occurrences >3-times). The performance of original dataset ( $n = 61$ ) was poor ( $r^2 = 0.26$ ; RMSEP = 5.99). Then, we removed the samples whose residuals were 20% larger than the range of environmental gradient. After being screened ( $n = 43$ , including 32 wetlands, 5 forests, 5 grasslands, and 1 residence), the one-component WA-PLS model displayed better performance ( $r^2 = 0.52$ ; RMSEP = 3.39), which was selected for HII reconstruction as assessed by random  $t$ -test (Table 1; Figure 4). Additionally, the standard error estimated by WA-PLS component one for HII reconstruction was 1.04.

### 3.3 | Fossil pollen assemblages from the TQ1 profile

A total of 33 pollen types were identified in 24 samples of TQ1 profile, consisting of 9 tree types, 4 shrub types, 19 herb types, and *Sphagnum*. Trees pollen taxa were mainly consisted of *Betula* (17.1%–51.0%), *Pinus* (8.3%–40.7%), *Larix* (4.2%–18.2%), and *Alnus* (2.7%–18.1%); shrub pollen taxa were mainly from Ericaceae (0.7%–14.7%) and *Salix* (0.2%–7.4%); herb pollen taxa were dominated by Cyperaceae (0.2%–13.9%), *Artemisia* (1.8%–7.9%), Poaceae (0.2%–5.5%), and Chenopodiaceae (0.2%–3.3%); the content of *Sphagnum* was 1.6%–48.8%. Pollen concentrations ranged between  $1.1 \times 10^4$

	Component	RMSEP	$r^2$	Ave. bias	Max. bias	Rand. t-test
a	<b>WA-PLS (component 1)</b>	<b>5.988</b>	<b>0.260</b>	<b>0.179</b>	<b>11.822</b>	–
	WA-PLS (component 2)	5.155	0.451	0.039	9.905	0.693
	WA-PLS (component 3)	4.791	0.526	0.022	9.162	0.754
	WA-PLS (component 4)	4.579	0.567	0.086	8.236	0.595
	WA-PLS (component 5)	4.472	0.587	0.073	7.402	0.852
b	<b>WA-PLS (component 1)</b>	<b>3.390</b>	<b>0.520</b>	<b>0.014</b>	<b>4.516</b>	–
	WA-PLS (component 2)	2.854	0.659	–0.035	4.528	0.853
	WA-PLS (component 3)	2.698	0.695	–0.045	4.201	0.943
	WA-PLS (component 4)	2.642	0.707	–0.028	4.026	1.000
	WA-PLS (component 5)	2.609	0.715	–0.047	4.086	1.000

**TABLE 1** Performance statistics of weighted averaging partial least squares (WA-PLS) models between pollen and Human Influence Index (HII)

Note: the chosen model is marked in bold. a: original dataset,  $n = 61$ ; b: screened dataset,  $n = 43$

and  $4.5 \times 10^5$  grains/g. Only the most abundant taxa were shown in Figure 5. The pollen assemblages of TQ1 profile were divided into three zones based on CONISS analysis.

### 3.3.1 | Zone 1 (24–15 cm): 1860–1920 AD

*Pinus*, *Betula*, *Larix*, and *Alnus* dominated, coniferous pollen proportions ranged from 39% to 54%, broad-leaved trees pollen percentages fluctuated between 21.4% and 33.9%. The content of shrub pollen was 3.2%–9.7%. Herb pollen content was 14.4%–26%, predominated by Cyperaceae pollen (4.8%–13.9%), with some *Artemisia* (3%–7.2%) and Poaceae pollen (1.5%–5.5%). The proportion of *Sphagnum* spores was 10.2%–37.7%, AP/NAP was 2.1–4.5, and the total pollen concentrations ranged from  $2.9 \times 10^4$  to  $4.5 \times 10^5$  grains/g. Reconstructed historical HII in Tuqiang profile ranged from 12.0 to 13.0 (average 12.7).

### 3.3.2 | Zone 2 (15–10 cm): 1920–1980 AD

Coniferous pollen percentages (37.7%–46.2%) decreased, while broad-leaved trees pollen proportion (28%–39.4%) increased gradually. *Pinus* pollen content was 23.9%–30%; *Betula* pollen proportion was 23.1%–31.1%. Shrubs pollen content (6.2%–11.6%) increased, herbs pollen content (9.7%–19.6%) decreased, and the contents of Cyperaceae and Poaceae were 3.8%–8.9% and 0.5%–2.2%, respectively. The content of *Artemisia* and Chenopodiaceae was 4.6%–7.9% and 0.2%–2.4%, respectively. *Sphagnum* spores content was 27.2%–48.8%, AP/NAP was 2.9–4.0, and total pollen concentration was  $3.6 \times 10^4$ – $1.9 \times 10^5$  grains/g. Reconstructed historical HII values were 8.4–13.6 (average 10.9).

### 3.3.3 | Zone 3 (above 10 cm): Since 1980 AD

The percentages of broad-leaved trees pollen (50.9%–64.8%) increased markedly, especially *Betula* and *Alnus*, the content of *Betula*

(39.6%–51%) and *Alnus* (9.1%–18.1%) peaked in the entire profile. The percentages of conifers (18.4%–32.2%) dropped sharply; the proportion of Ericaceae (2.2%–14.7%) increased distinctly. The content of herbs (5.7%–11.8%) reduced substantially, such as Cyperaceae (0.2%–2.9%) and Poaceae (0.2%–1.8%), while Chenopodiaceae (0.4%–3.3%) and *Aster* (0%–0.7%) proportions increased. The proportion of *Sphagnum* spores was 1.6–8.7%, AP/NAP was 2.8–6.8, and the total pollen concentrations exhibit a drastic reduction ( $1.1 \times 10^4$ – $2.4 \times 10^4$  grains/g). Reconstructed HII values were 7.6–12.7 (average 9.6).

## 4 | DISCUSSION

### 4.1 | Relationships between surface pollen assemblages and environmental variables

The relationships among modern pollen, climate, and human activities are the basis for improving the interpretation of fossil pollen records. It is important to assess the relations of modern pollen to environment. The relationships between surface pollen assemblages and environmental variables were well investigated by using RDA ordination (Figure 3). Tann and Pann negatively correlated to *Larix*, *Pinus*, *Betula*, *Alnus*, and Ericaceae, which dominated at forests and wetlands in the Greater Khingan Mountains, and positively correlated to *Quercus*, Cyperaceae, and *Sanguisorba*. Strong positive correlations occurred between HII and human-companion pollen types, such as Polygonaceae, *Artemisia*, Chenopodiaceae, *Aster*, and *Taraxacum* (Figure 3), which agreed with the findings from Y. Zhang et al. (2010) and H. Huang et al. (2018). In RDA analysis three variables (HII, Tann, and Pann) captured 3.69%, 20.14%, and 6.40% of the total variance in pollen distributions, respectively. The dominant factor that influenced the distribution of surface pollen assemblages among different land-use types in the Greater Khingan Mountains was Tann, then Pann and HII. M. Y. Li et al. (2012) also suggested that pollen assemblages were mainly controlled by temperature in Northeast China. Geng et al. (2019) indicated that the mean temperature of the coldest month was the most significant driver influencing modern pollen

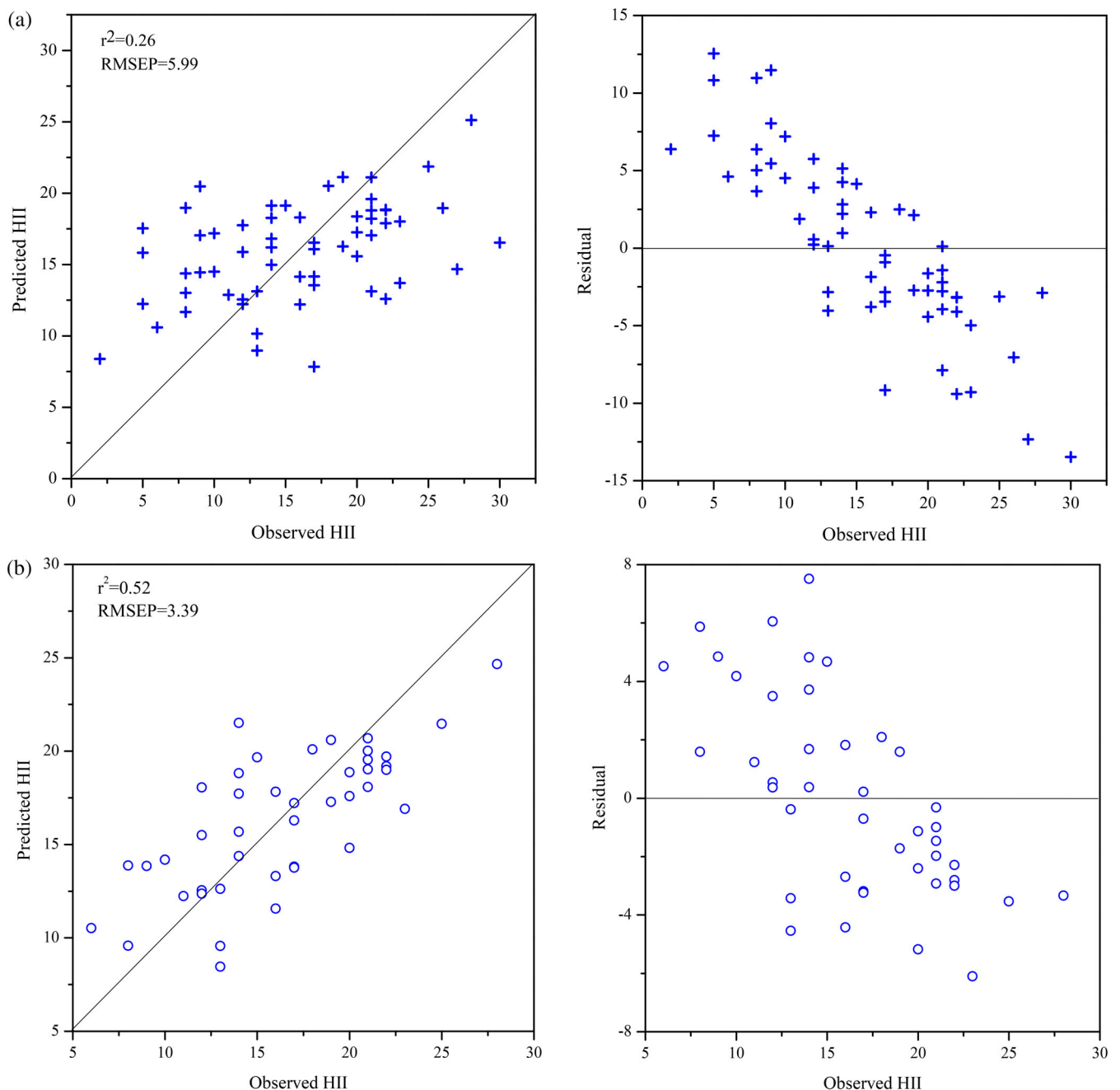


**FIGURE 4** Scatter plots of observed Human Influence Index (HII) versus weighted averaging partial least squares (WA-PLS) predicted HII values and residuals based on surface soil pollen samples. (a) Original dataset,  $n = 61$ ; (b) screened dataset,  $n = 43$  [Colour figure can be viewed at [wileyonlinelibrary.com](http://wileyonlinelibrary.com)]

assemblages in Northeast China. Therefore, our results indicated that modern pollen assemblages from different land-use types in the Greater Khingan Mountains potentially enable to quantitatively reconstruct HII, Tann, and Pann.

#### 4.2 | Influencing factor of vegetation variation in Tuqiang peatland

Novorotskii (2007) showed the long-period changes in annual mean air temperature ( $^{\circ}\text{C}$ ) and annual precipitation totals (% the ratio to the

mean of 1961–1990 AD) in the Amur River basin from 1891 to 2004 AD (Figure 6). The climate was cold (temperature fluctuated from  $-1.4$  to  $-0.2^{\circ}\text{C}$ , average  $-0.8^{\circ}\text{C}$ ) and dry (the precipitation totals were 79.8%–114%, average 91.8%) during the period of 1900–1920 AD; it was relative warm (temperature ranged from  $-1.4$  to  $0.9^{\circ}\text{C}$ , average  $-0.3^{\circ}\text{C}$ ) and moist (the precipitation totals were 85.5%–110%, average 96.9%) from 1930 to 1950 AD; the temperature declined after 1950 AD (from  $-1.5$  to  $-0.2^{\circ}\text{C}$ , average  $-0.6^{\circ}\text{C}$ ) and then increased since 1970 AD (temperature fluctuated from  $-0.7$  to  $1.6^{\circ}\text{C}$ , average  $0.4^{\circ}\text{C}$ ); it was the moistest period around 1960 AD (the precipitation totals were 102%–119%, average 109.1%) and



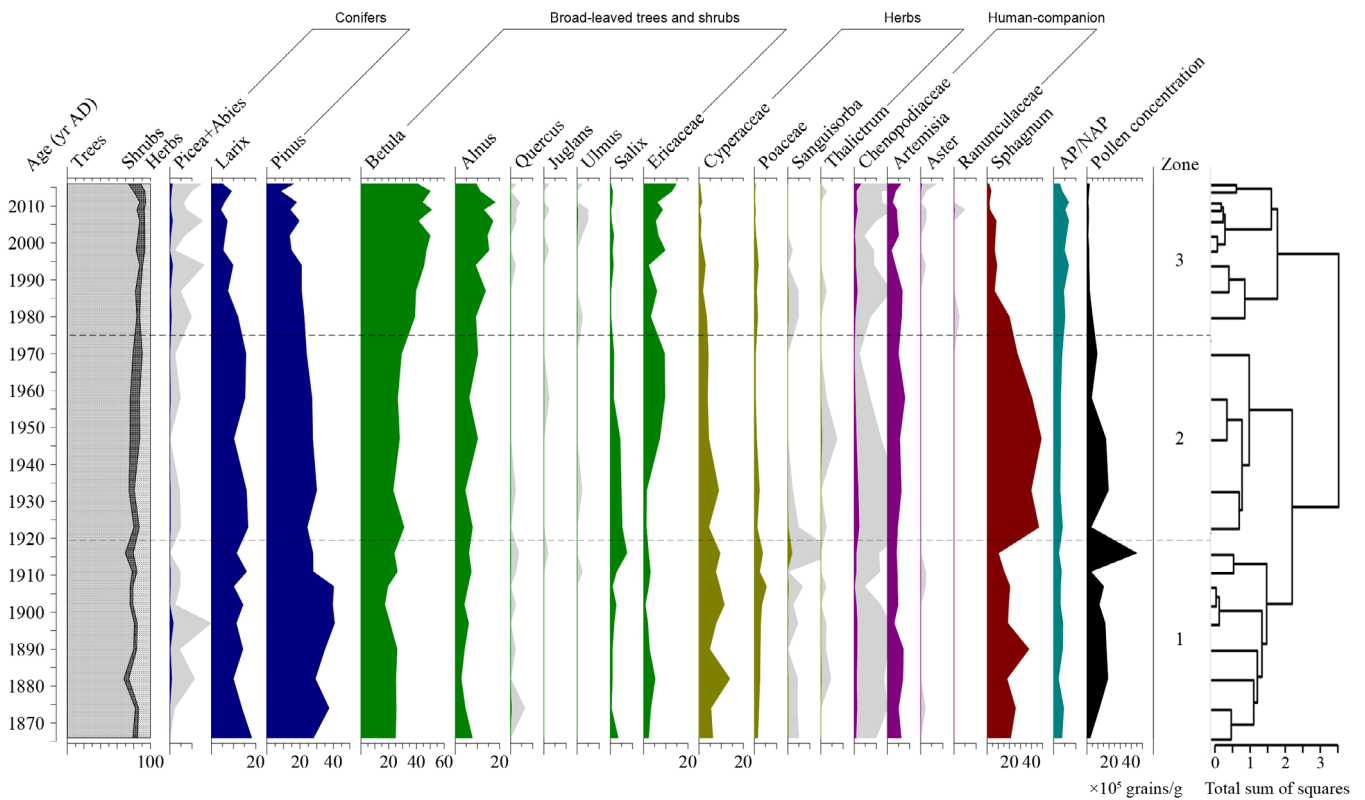


**FIGURE 5** Pollen diagram of TQ1 profile during the last 150 years. The abundances of pollen species were expressed as percentages. The grey shading represents an exaggeration of 10 times of the original data [Colour figure can be viewed at [wileyonlinelibrary.com](http://wileyonlinelibrary.com)]

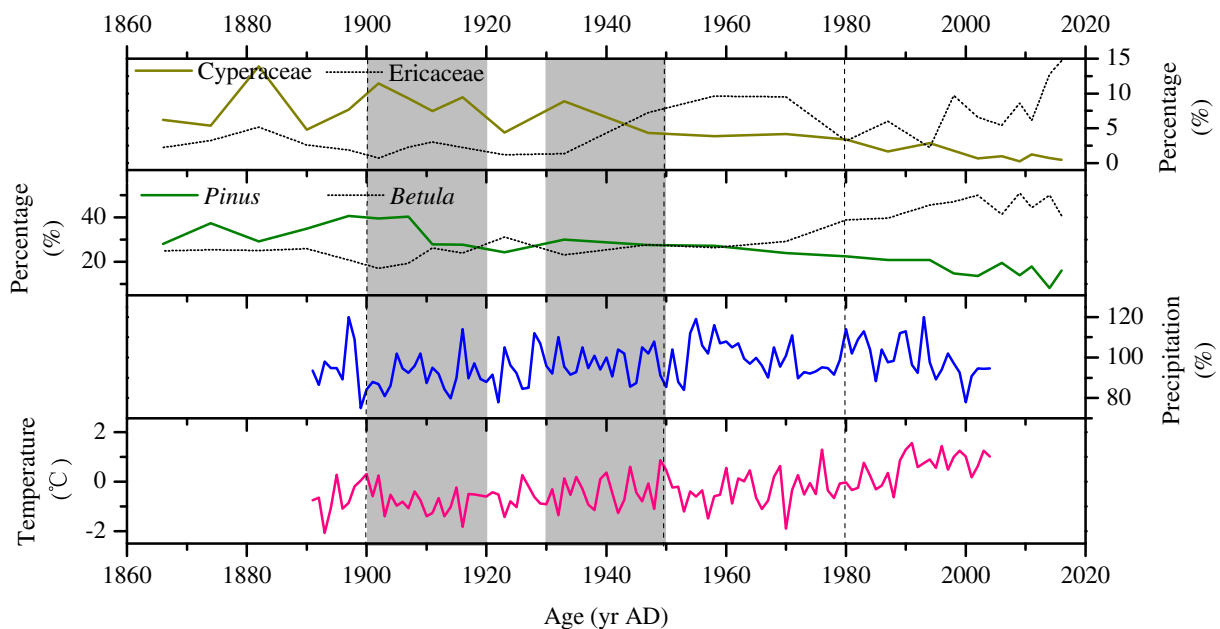


**FIGURE 6** The percentage curves of *Cyperaceae*, *Ericaceae*, *Pinus*, and *Betula* from TQ1 profile. Changes in annual mean air temperature ( $^{\circ}\text{C}$ ) and annual precipitation totals (% the ratio to the mean of 1961–1990) in the Amur River basin (Novorotskii, 2007). The grey bars represent the period of abnormal reduction of *Pinus* and *Cyperaceae* [Colour figure can be viewed at [wileyonlinelibrary.com](http://wileyonlinelibrary.com)]

became drying at 1970 AD (the precipitation totals were 89.8%–98.8%, average 93.5%) and, then, became moist after 1980 AD (the precipitation totals were 88.4%–120%, average 101.9%) and became dry again since 2000 AD (the precipitation totals were 77.9%–94.7%, average 90.5%).

During the period from 1860 to 1900 AD, the contents of *Cyperaceae* and *Pinus* were relatively high. The percentage of cold-tolerant *Pinus* around Tuqiang peatland was the highest (Figures 5 and 6) from 1900 to 1910 AD when the climate was relatively cold and dry (average temperature,  $-0.7^{\circ}\text{C}$ ; average precipitation totals,

92.7%) (Novorotskii, 2007). *Pinus* could indicate low-temperature environment (Yao et al., 2017). It was worth noting that the content of cold-tolerant *Pinus* declined sharply with the expansion of birch secondary forest after 1910 AD, though the climate was coldest (average temperature was  $-0.8^{\circ}\text{C}$ ) during the period of 1900–1920 AD. Stebich et al. (2015) implied the expansion of birch forests at the cost of pine forest denoting substantial ecosystem disturbances. C. H. Li et al. (2011) and Mackenzie et al. (2018) also interpreted that logging could lead to secondary birch forests expand. A selective logging may have occurred around Tuqiang peatland since around 1910 AD. After 1920 AD, the climate became warmer and wetter (Figure 6); the content of hygrophilic Cyperaceae decreased obviously with the invasion of drought-tolerance brush (Ericaceae) though the climate was moist during the period of 1930–1950 AD (average precipitation totals, 96.9%), especially after 1980 AD (average precipitation totals, 101.9%). Humid environment is conducive to the development of peatlands, while intensified human influence might result in the degradation of peatlands. Yu et al. (2017) demonstrated that high content of Cyperaceae represented a high moisture level, and the content of Cyperaceae might be positively related to health or extent of peatlands. The reduction of hygrophilous Cyperaceae, which was the major component of vegetation in the peatland, reflects a decrease of water level. Additionally, brush invasion reveals the degradation of peatland with a drying tendency. We inferred that the abnormal reduction of Cyperaceae and *Pinus* might

be mainly caused by human disturbance rather than by climate during the past 150 years in Tuqiang peatland.

### 4.3 | Human activities in Greater Khingan Mountains during the last 150 years

Deforestation is one of the most direct and immediate ways for human settlement and land reclamation in early agricultural period (M. Y. Li et al., 2015; L. Zhao et al., 2017). Variations of arboreal taxa and cereal Poaceae pollen contents are commonly regarded as direct evidence of human influence (J. Y. Li et al., 2014; M. Y. Li et al., 2015). The presence of human-companion plants (e.g., Chenopodiaceae and *Artemisia*) also indicates anthropogenic activities (M. Y. Li et al., 2015; H. Y. Liu et al., 2006; Stebich et al., 2015; H. Zhang et al., 2015). As we know, the Greater Khingan Mountains have a high percentage of forest cover due to its higher elevation; the main human disturbance is deforestation (e.g., logging and fire) (Gao et al., 2018). As we could see in Figure 7, the quantitatively reconstructed HII values in Tuqiang peatland over the past 150 years show a good correspondence with the percentage curve of human-companion Chenopodiaceae. We compared the reconstructed HII values in Tuqiang peatland with forest cutting area and wood production in Greater Khingan Mountains (G. Z. Liu, 2001) and the historical population in Heilongjiang Province (Cong et al., 2016), we also selected some proxies which reflected fire

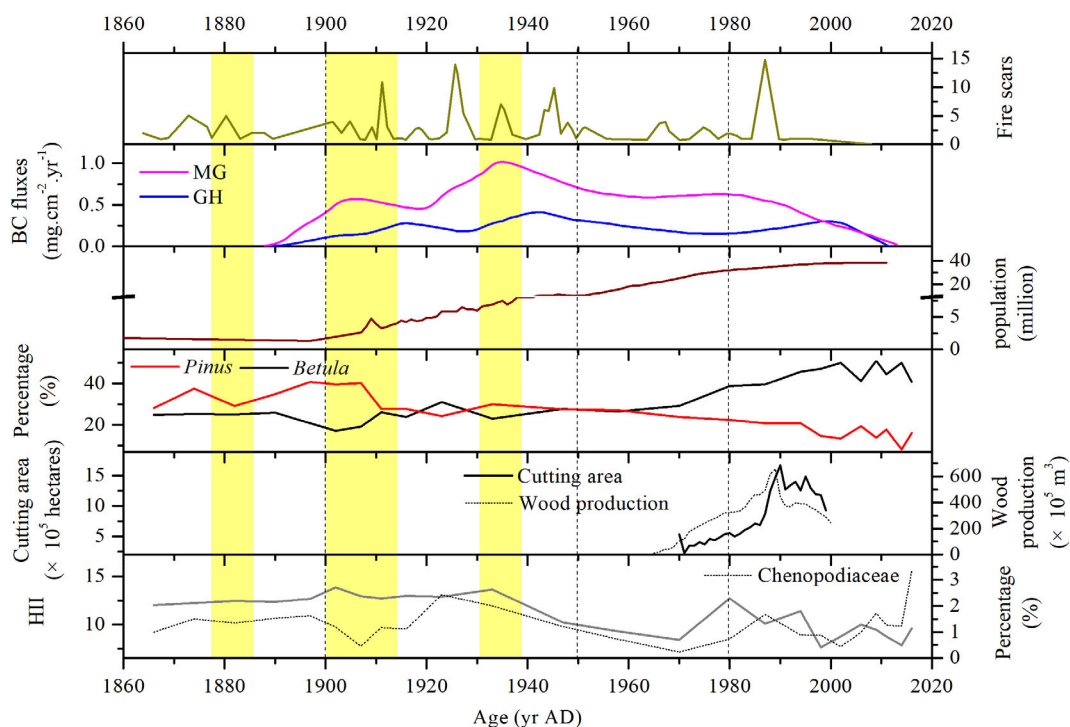


**FIGURE 7** Comparison of reconstructed Human Influence Index (HII) values, percentages of *Pinus*, *Betula*, and Chenopodiaceae in Tuqiang peatland with other proxy records. Fire scars numbers in the northern part of the Greater Khingan Mountains (Lu, 2012), average deposition fluxes of black carbon (BC) in Greater Khingan Mountains (MG: Mangui; GH: Genhe) (Gao et al., 2018), the historical population in Heilongjiang Province (Cong et al., 2016), forest cutting area, and wood production in the Greater Khingan Mountains (G. Z. Liu, 2001). The yellow bars represent the period of higher human disturbance [Colour figure can be viewed at [wileyonlinelibrary.com](http://wileyonlinelibrary.com)]

frequency and intensity in other published studies, such as the number of fire scars from tree-ring records and the average deposition fluxes of black carbon (BC) in the north part of the Greater Khingan Mountains (Gao et al., 2018; Lu, 2012).

During the period of 1860–1900 AD, the reconstructed HII values indicate that human activities intensity increased gradually in Tuqiang peatland. As we know that the population in Heilongjiang Province was only around 2 million before 1900 AD (Cong et al., 2016), the native inhabitants remained their primitive hunt, gathering activities and human interference were weak. Lu (2012) revealed lower intensity and frequency of fire events (few numbers of fire scars) in the north part of Greater Khingan Mountains at the same period. Gao et al. (2018) also indicated lower average deposition fluxes of BC in Mangui (MG) and Genhe (GH) and suggested that fire events were mainly generated by natural factors such as lightning before 1900 AD in Greater Khingan Mountains. In the spring of 1882 AD, hunters found gold accidentally in Mohe area, northern of the Greater Khingan Mountains (Lu, 2012). Placer gold mining attracted large numbers of human beings migrating to the north of the Greater Khingan Mountains. Tuqiang peatland was only 33 km apart from Mohe county; increase in population led to an increasing trend of human influence since 1882 AD. Placer gold mining damaged bogs, floodplains, as well as various forest communities in the Greater Khingan Mountains, which resulted in large-scale soil erosion and affected the balance of ecosystem seriously (Egidareva & Simonovb, 2015).

The reconstructed historical HII values steadily increased since 1900 AD and reached peak values at around 1930 AD. The Greater Khingan Mountains were exploited by Russian forces through wars, which caused large numbers of refugees moved north to Heilongjiang Province at 1900 AD. Additionally, a large immigration event occurred from 1907 to 1911 AD and the population in Heilongjiang Province up to 4 million (Cong et al., 2016; Lu, 2012). People cleared vegetation (e.g., felled trees) and developed lands to meet their daily needs (e.g., building settlements) when migrated to a new area, the obviously increasing population of Heilongjiang Province caused intensified human impacts (D. B. Li & Shi, 1987; Sun, 1983). Besides, owing to the construction of Chinese Eastern Railway by Russian at 1897 AD, the forests along and near the railroad tracks were cut down for railroad ties, building houses, and fuels. Our pollen record marked a sharp reduction of *Pinus* percentage between 1900 and 1920 AD (Figure 7). Large-scale land reclamation and deforestation destroyed forest vegetation landscape and led to soil erosion and degradation. Lu (2012) and Cong et al. (2016) recorded another immigration and the population in Heilongjiang Province up to 6 million from 1920 to 1930 AD, the increased population led to intensified human disturbance. The deposition fluxes of BC in MG and GH and the number of fire scars in the north of the Greater Khingan Mountains also exhibited peak values at this period, which marked strengthened fire frequency and intensity (Gao et al., 2018; Lu, 2012). In Figure 7, the percentage of *Pinus* in our study decreased since about 1930 AD. G. Z. Liu (2001) recorded that Japanese invaders plundered forest resources without limit, and over 723,000 cubic metres of forests were harvested

annually in the Greater Khingan Mountains during the period of Manchukuo (1931–1945 AD). By the time of 1945 AD, Japanese invaders had plundered more than 5 million cubic metres of timber (mostly *Pinus sylvestris*) from the Greater Khingan Mountains (G. Z. Liu, 2001).

From 1950 to 1980 AD, the reconstructed HII values of Tuqiang peatland declined and remained a low level. After the founding of new China (1949 AD), Chinese government carried out three consecutive large-scale developments and constructions in Greater Khingan Mountains at 1955, 1958, and 1964 AD, respectively. Our pollen assemblages recorded these three logging events (reduction of *Pinus* with the expansion of *Betula*) between 1950 and 1980 AD (Figure 7). The expanding of birch forest at the expense of pine may denote ecosystem disturbances (Stebich et al., 2015). Mackenzie et al. (2018) also suggested logging led to the expansion of secondary birch forests. From the perspective of landscape ecology, the three forest developments and constructions led to the increase of patch fragmentation, which affected the spread of medium- and low-intensity fires in forest areas to some extent. Lu (2012) and Gao et al. (2018) also suggested the declined number of fire scars and the deposition fluxes of BC in the Greater Khingan Mountains, suggesting a reduction of intensity and frequency of fire events after 1950 AD. In addition, the annual forest cutting area and wood production suggested an increasing trend from 1970 to 1990 AD (G. Z. Liu, 2001); our reconstructed HII values also indicated a strengthened human disturbance intensity since 1970 AD.

Since 1980 AD, the reconstructed HII values remained a higher level though with fluctuation in Tuqiang peatland. The Chinese Government paid more attention to forest resources protection and introduced new policies of forest protection in the Greater Khingan Mountains, allowing the region to be friendly exploited with planning after 1980 AD (G. Z. Liu, 2001). In addition, with the implementation of fire prevention policies (e.g., forest firefighting brigade and establish fire monitoring stations), people's awareness of fire prevention had been improved greatly. Lu (2012) and Gao et al. (2018) marked decreased number of fire scars and the deposition fluxes of BC in the Greater Khingan Mountains, suggesting a reduction of intensity and frequency of fire events after 1980 AD. Though with the forest protection and fire prevention, the population of Heilongjiang Province increased close to 40 million in the 21st century (Cong et al., 2016), and anthropogenic activities increased again with the needs of economic development in the current time.

## 5 | CONCLUSIONS

Pollen assemblages from Tuqiang peatland provided a historical vegetation record with high resolution over the last 150 years. Quantitative reconstruction of HII values based on pollen-HII calibration model showed that both anthropogenic activities and climate change influenced vegetation and environment of peatland. In the context of the global warming, the development and degradation of peatland were affected more by human activities. Placer gold mining, war, and immigration all led to the expansion of population in Heilongjiang

Province; the intensity of human influence gradually strengthened from 1860 to 1950 AD. The percentage of Cyperaceae decreased while the content of Ericaceae increased obviously since 1930 AD; widescale land reclamation and deforestation led to degradation of peatland. The Chinese Government implemented forest protection policies to protect forest resources and allowed planned exploitation in the Greater Khingan Mountains after the foundation of new China; the intensity of human impact declined clearly. Since 1980 AD to present, increasing cutting area for wood production (*Pinus* decreased), has exacerbated the degradation of peatland (Ericaceae increased). To meet the needs of economic development, human disturbance increased again, which should be noticed. In future, further palaeoenvironmental studies of quantitatively reconstruct climate and human impact in late Holocene in the Greater Khingan Mountains are required, for the purpose of a better understanding of the interaction between natural climate and anthropogenic activities.

## ACKNOWLEDGMENTS

The authors gratefully acknowledge the assistance of the Analysis and Test Center of the Northeast Institute of Geography and Agroecology (IGA) of the Chinese Academy of Sciences (CAS). This work was supported by the National Key Research and Development Project (Grant No. 2016YFA0602301), the National Natural Science Foundation of China (Grant No. 42171103, 42101108, 41911530188), the China Postdoctoral Science Foundation (Grant No. 2020M681059), the Youth Innovation Promotion Association CAS (No. 2020235), the Fundamental Research Funds for the Central Universities (Grant No. 2412019BJ003), and the Jilin Provincial Department of Science and Technology (Grant No. 20190101011JH).

## DATA AVAILABILITY STATEMENT

The data that support the findings of this study are available from the corresponding author upon reasonable request.

## ORCID

Chuanyu Gao  <https://orcid.org/0000-0003-2792-5022>

Guoping Wang  <https://orcid.org/0000-0002-8350-812X>

## REFERENCES

- Appleby, P. G., & Oldfield, F. (1978). The calculation of lead-210 dates assuming a constant rate of supply of unsupported  $^{210}\text{Pb}$  to the sediment. *Catena*, 5, 1–8. [https://doi.org/10.1016/S0341-8162\(78\)80002-2](https://doi.org/10.1016/S0341-8162(78)80002-2)
- Cheng, Z. J., Weng, C. Y., Steinke, S., & Mohtadi, M. (2018). Anthropogenic modification of vegetated landscapes in southern China from 6,000 years ago. *Nature Geoscience*, 11, 939–943. <https://doi.org/10.1038/s41561-018-0250-1>
- Cong, J. X., Gao, C. Y., Han, D. X., Liu, H. X., & Wang, G. P. (2019). History metal (Pb, Zn, and Cu) deposition and Pb isotope variability in multiple peatland sites in the northern Great Hinggan Mountains, Northeast China. *Environmental Science and Pollution Research*, 26, 21784–21796. <https://doi.org/10.1007/s11356-019-04432-7>
- Cong, J. X., Gao, C. Y., Zhang, Y., Zhang, S. Q., He, J. B., & Wang, G. P. (2016). Dating the period when intensive anthropogenic activity began to influence the Sanjiang Plain, Northeast China. *Scientific Reports*, 6, 22153. <https://doi.org/10.1038/srep22153>
- Crutzen, P. J. (2002). Geology of mankind. *Nature*, 415, 23. <https://doi.org/10.1038/415023a>
- Crutzen, P. J., & Stoermer, E. F. (2000). The ‘Anthropocene’. *IGBP Newsletter*, 41, 17–18.
- Dixit, S. S., Cumming, B. F., Birks, H. J. B., Smol, J. P., Kingston, J. C., Uutala, A. J., Charles, D. F., & Camburn, K. E. (1993). Diatom assemblages from Adirondack lakes (New York, USA) and the development of inference models for retrospective environmental assessment. *Journal of Paleolimnology*, 8, 27–47. <https://doi.org/10.1007/BF00210056>
- Egidareva, E. G., & Simonovb, E. A. (2015). Assessment of the environmental effect of placer gold mining in the Amur River basin. *Water Resources*, 42, 897–908. <https://doi.org/10.1134/S0097807815070039>
- Fægri, K., & Iversen, J. (1989). *Textbook of pollen analysis* (4th ed.). John Wiley and Sons.
- Fick, S. E., & Hijmans, R. J. (2017). Worldclim 2: New 1-km spatial resolution climate surfaces for global land areas. *International Journal of Climatology*, 37, 4302–4315. <https://doi.org/10.1002/joc.5086>
- Gao, C. Y., He, J. B., Cong, J. X., Zhang, S. Q., & Wang, G. P. (2018). Impact of forest fires generated black carbon deposition fluxes in the Great Hinggan Mountains (China). *Land Degradation & Development*, 29(7), 2073–2081. <https://doi.org/10.1002/ldr.2837>
- Geng, R. W., Zhao, Y., Cui, Q. Y., & Qin, F. (2019). Representation of modern pollen assemblages with respect to vegetation and climate in Northeast China. *Quaternary International*, 532, 126–137. <https://doi.org/10.1016/j.quaint.2019.11.003>
- Han, D. X., Gao, C. Y., Li, Y. H., Liu, H. X., Cong, J. X., Yu, X. F., & Wang, G. P. (2020). Potential in paleoclimate reconstruction of modern pollen assemblages from natural and human-induced vegetation along the Heilongjiang River basin, NE China. *Science of the Total Environment*, 745, 141121. <https://doi.org/10.1016/j.scitotenv.2020.141121>
- Han, D. X., Gao, C. Y., Yu, Z. C., Yu, X. F., Li, Y. H., Cong, J. X., & Wang, G. P. (2019). Late Holocene vegetation and climate changes in the Great Hinggan Mountains, Northeast China. *Quaternary International*, 532, 138–145. <https://doi.org/10.1016/j.quaint.2019.11.017>
- Huang, X. Z., Chen, X. M., & Du, X. (2018). Modern pollen assemblages from human-influenced vegetation in northwestern China and their relationship with vegetation and climate. *Vegetation History and Archaeobotany*, 27, 767–780. <https://doi.org/10.1007/s00334-018-0672-0>
- Li, C. H., Wu, Y. H., & Hou, X. H. (2011). Holocene vegetation and climate in Northeast China revealed from Jingbo Lake sediment. *Quaternary International*, 229(1), 67–73. <https://doi.org/10.1016/j.quaint.2009.12.015>
- Li, D. B., & Shi, F. (1987). *Summary of immigration in Heilongjiang Province*. Harbin: Heilongjiang People's Publishing House (in Chinese).
- Li, J. Y., Dodson, J., Yan, H., Zhang, D. D., Zhang, X. J., Xu, Q. H., Lee, H. F., Pei, Q., Cheng, B., Li, C., Ni, J., Sun, A., Lu, F., & Zong, Y. Q. (2017). Quantifying climatic variability in monsoonal northern China over the last 2200 years and its role in driving Chinese dynastic changes. *Quaternary Science Reviews*, 159, 35–46. <https://doi.org/10.1016/j.quascirev.2017.01.009>
- Li, J. Y., Xu, Q. H., Gaillard-Lemdhahl, M. J., Seppä, H., Li, Y. C., Hun, L. Y., & Li, M. Y. (2013). Modern pollen and land-use relationships in the Taihang Mountains, Hebei Province, northern China—a first step towards quantitative reconstruction of human-induced land cover changes. *Vegetation History and Archaeobotany*, 22(6), 463–477. <https://doi.org/10.1007/s00334-013-0391-5>
- Li, J. Y., Zhao, Y., Xu, Q. H., Zheng, Z., Lu, H. Y., Luo, Y. L., Li, Y., Li, C., & Seppä, H. (2014). Human influence as a potential source of bias in pollen-based quantitative climate reconstructions. *Quaternary Science Reviews*, 99, 112–121. <https://doi.org/10.1016/j.quascirev.2014.06.005>
- Li, M. Y., Li, Y. C., Xu, Q. H., Pang, R. M., Ding, W., Zhang, S. R., & He, Z. G. (2012). Surface pollen assemblages of human-disturbed vegetation



- and their relationship with vegetation and climate in Northeast China. *Chinese Science Bulletin*, 57, 535–547. <https://doi.org/10.1007/s11434-011-4853-9>
- Li, M. Y., Xu, Q. H., Zhang, S. R., Li, Y. C., Ding, W., & Li, J. Y. (2015). Indicator pollen taxa of human-induced and natural vegetation in Northern China. *The Holocene*, 25(4), 686–701. <https://doi.org/10.1177/0959683614566219>
- Li, X. Q., Shang, X., Dodson, J., & Zhou, X. Y. (2009). Holocene agriculture in the Guanzhong basin in NW China indicated by pollen and charcoal evidence. *The Holocene*, 19(8), 1213–1220. <https://doi.org/10.1177/0959683609345083>
- Liu, G. Z. (2001). *Chronicles of the Greater Khingan Mountains*. Beijing: Fangzhi Publishing Press (in Chinese).
- Liu, H. X., Yu, Z. C., Han, D. X., Gao, C. Y., Yu, X. F., & Wang, G. P. (2019). Temperature influence on peatland carbon accumulation over the last century in Northeast China. *Climate Dynamics*, 53, 1–13. <https://doi.org/10.1007/s00382-019-04813-1>
- Liu, H. Y., Wang, Y., Tian, Y. H., Zhu, J. L., & Wang, H. Y. (2006). Climatic and anthropogenic control of surface pollen assemblages in East Asian steppes. *Review of Palaeobotany and Palynology*, 138, 281–289. <https://doi.org/10.1016/j.revpalbo.2006.01.008>
- Lu, Y. X. (2012). *Tree-ring reconstructions of fire history and their relationships with human activities in Daxing'an Mountains*. Harbin, China (Master dissertation Northeast Forestry University) (in Chinese).
- Ma, L. S., Gao, C. Y., Kattel, G. R., Yu, X. F., & Wang, G. P. (2018). Evidence of diatom-inferred Holocene water level change and the evolution of Honghe Peatland in Sanjiang Plain, Northeast China. *Quaternary International*, 476, 82–94. <https://doi.org/10.1016/j.quaint.2018.02.025>
- Mackenzie, L., Bao, K. S., Mao, L. M., Klamt, A. M., Pratte, S., & Shen, J. (2018). Anthropogenic and climate-driven environmental change in the Songnen Plain of northeastern China over the past 200 years. *Palaeogeography, Palaeoclimatology, Palaeoecology*, 511, 208–217. <https://doi.org/10.1016/j.palaeo.2018.08.005>
- Melles, M., Svendsen, J. I., Fedorov, G., & Wagner, B. (2019). Northern Eurasian lakes-late Quaternary glaciation and climate history-introduction. *Boreas*, 48, 269–272. <https://doi.org/10.1111/bor.12395>
- Novorotskii, P. V. (2007). Climate changes in the Amur River basin in the last 115 years. *Russian Meteorology and Hydrology*, 32(2), 102–109. <https://doi.org/10.3103/S1068373907020045>
- Sanderson, E. W., Jaiteh, M., Levy, M. A., Redford, K. H., Wannebo, A. V., & Woolmer, G. (2002). The human footprint and the last of the wild. *Bioscience*, 52(10), 891–904. [https://doi.org/10.1641/0006-3568\(2002\)052\[0891:THFATL\]2.0.CO;2](https://doi.org/10.1641/0006-3568(2002)052[0891:THFATL]2.0.CO;2)
- Shu, J. W., Wang, W. M., Jiang, L. P., & Takahara, H. (2010). Early Neolithic vegetation history, fire regime and human activity at Kuahuqiao, Lower Yangtze River, East China: New and improved insight. *Quaternary International*, 227, 10–21. <https://doi.org/10.1016/j.quaint.2010.04.010>
- Stebich, M., Rehfeld, K., Schlütz, F., Tarasov, P. E., Liu, J. Q., & Mingram, J. (2015). Holocene vegetation and climate dynamics of NE China based on the pollen record from Sihailongwan Maar Lake. *Quaternary Science Reviews*, 124, 275–289. <https://doi.org/10.1016/j.quascirev.2015.07.021>
- Sun, Z. W. (1983). *Historical exploration of Heilongjiang Province*. Harbin: Heilongjiang People's Publishing House (in Chinese).
- Tang, L. Y., Mao, L. M., Shu, J. W., Li, C. H., Shen, C. M., & Zhou, Z. Z. (2016). *An illustrated handbook of quaternary pollen and spores in China*. Science Press (in Chinese).
- Ter Braak, C. J. F., & Juggins, S. (1993). Weighted averaging partial least squares regression (WA-PLS): An improved method for reconstructing environmental variables from species assemblages. *Hydrobiologia*, 269(270), 485–502. <https://doi.org/10.1007/BF00028046>
- Ter Braak, C. J. F., & Prentice, I. C. (1988). A theory of gradient analysis. *Advances in Ecological Research*, 18, 271–317. [https://doi.org/10.1016/S0065-2504\(08\)60183-X](https://doi.org/10.1016/S0065-2504(08)60183-X)
- Ter Braak, C. J. F., & Smilauer, P. (2003). *CANOCO Reference Manual and CanoDraw for Windows User's Guide: Software for Canonical Community Ordination* (Version 4.5). Microcomputer Power, Ithaca, NY.
- Van Cleef, D. J. (1994). Determination of  $^{226}\text{Ra}$  in soil using  $^{214}\text{Pb}$  and  $^{214}\text{Bi}$  immediately after sampling. *Health Physics*, 67, 288–289. <https://doi.org/10.1097/00004032-199409000-00012>
- van der Voet, H. (1994). Comparing the predictive accuracy of models using a simple randomization test. *Chemometrics and Intelligent Laboratory Systems*, 25, 313–323. [https://doi.org/10.1016/0169-7439\(94\)85050-x](https://doi.org/10.1016/0169-7439(94)85050-x)
- Wang, F. X., Qian, N. F., Zhang, Y. L., & Yang, H. Q. (1995). *Pollen flora of China*. Beijing: Science Press (in Chinese).
- WCS/CIESIN. (2005). Last of the Wild Data Version 2: Global Human Influence Index (HII). Wildlife Conservation Society (WCS) and Center for International Earth Science Information Network (CIESIN). Retrieved from <http://sedac.ciesin.columbia.edu/data/set/wildareas-v2-human-influence-index-geographic>
- Xing, W., Bao, K. S., Gallego-Sala, A. V., Charman, D. J., Zhang, Z. Q., Gao, C. Y., Lu, X., & Wang, G. P. (2015). Climate controls on carbon accumulation in peatlands of Northeast China. *Quaternary Science Reviews*, 115(9), 78–88. <https://doi.org/10.1016/j.quascirev.2015.03.005>
- Xu, Q. H., Xiao, J. L., Li, Y. C., Tian, F., & Nakagawa, T. (2010). Pollen-based quantitative reconstruction of Holocene climate changes in the Daihai Lake area, Inner Mongolia, China. *Journal of Climate*, 23(11), 2856–2868. <https://doi.org/10.1175/2009jcli3155.1>
- Yao, F. L., Ma, C. M., Zhu, C., Li, J. Y., Chen, G., Tang, L. Y., Huang, M., Jia, T., & Xu, J. J. (2017). Holocene climate change in the western part of Taihu Lake region, East China. *Palaeogeography, Palaeoclimatology, Palaeoecology*, 485, 963–973. <https://doi.org/10.1016/j.palaeo.2017.08.022>
- Yu, S. H., Zheng, Z., Kershaw, P., Skrypnikova, M., & Huang, K. Y. (2017). A late Holocene record of vegetation and fire from the Amur Basin, far-eastern Russia. *Quaternary International*, 432, 79–92. <https://doi.org/10.1016/j.quaint.2014.07.059>
- Zhang, H., Piilo, S. R., Amesbury, M. J., Charman, D. J., Gallego-Sala, A. V., & Väliranta, M. M. (2018). The role of climate change in regulating arctic permafrost peatland hydrological and vegetation change over the last millennium. *Quaternary Science Reviews*, 182, 121–130. <https://doi.org/10.1016/j.quascirev.2018.01.003>
- Zhang, H., Zhang, Y., Kong, Z. C., Yang, Z. J., Li, Y. M., & Tarasov, P. E. (2015). Late Holocene climate change and anthropogenic activities in North Xinjiang: Evidence from a peatland archive, the Caotanhu wetland. *The Holocene*, 25(2), 323–332. <https://doi.org/10.1177/0959683614558646>
- Zhang, Y., Kong, Z. C., Wang, G. H., & Ni, J. (2010). Anthropogenic and climatic impacts on surface pollen assemblages along a precipitation gradient in north-eastern China. *Global Ecology and Biogeography*, 19, 621–631. <https://doi.org/10.1111/j.1466-8238.2010.00534.x>
- Zhao, C., Li, X. Q., Zhou, X. Y., Zhao, K. L., & Yang, Q. (2015). Holocene vegetation succession and response to climate change on the south bank of the Heilongjiang-Amur River, Mohe County, Northeast China. *Advances in Meteorology*, 2016(12), 1–11. <https://doi.org/10.1155/2016/2450697>
- Zhao, L., Ma, C. M., Leipe, C., Long, T. W., Liu, K. B., Lu, H. Y., Tang, L., Zhang, Y., Wagner, M., & Tarasov, P. E. (2017). Holocene vegetation dynamics in response to climate change and human activities derived from pollen and charcoal records from southeastern China. *Palaeogeography, Palaeoclimatology, Palaeoecology*, 485, 644–660. <https://doi.org/10.1016/j.palaeo.2017.06.035>



Zhao, Y., Yu, Z. C., Liu, X. J., Zhao, C., Chen, F. H., & Zhang, K. (2010). Late Holocene vegetation and climate oscillations in the Qaidam basin of the northeastern Tibetan Plateau. *Quaternary Research*, 73(1), 59–69. <https://doi.org/10.1016/j.yqres.2008.11.007>

#### SUPPORTING INFORMATION

Additional supporting information may be found in the online version of the article at the publisher's website.

**How to cite this article:** Han, D., Gao, C., Liu, H., Li, Y., Cong, J., Yu, X., & Wang, G. (2021). Anthropogenic and climatic-driven peatland degradation during the past 150 years in the Greater Khingan Mountains, NE China. *Land Degradation & Development*, 1–13. <https://doi.org/10.1002/ldr.4036>